Electronic structure of Ti^{3+} in $BeAl_2O_4$

1992 J. Phys.: Condens. Matter 4 5181

(http://iopscience.iop.org/0953-8984/4/22/016)

J. Phys.: Condens. Matter 4 (1992) 5181–5188. Printed in the UK

Electronic structure of Ti^{3+} in $BeAl_2O_4$

Chuan-Yun Xiao†, Jin-Long Yang†‡, Shang-Da Xia§ and Ke-Lin Wang†

† Centre for Fundamental Physics, University of Science and Technology of China, Hefei, Anhui 230026, People's Republic of China

‡ CCAST (World Laboratory), PO Box 8730, Beijing 100080, People's Republic of China

§ Department of Physics, University of Science and Technology of China, Hefei, Anhui 230026, People's Republic of China

Received 28 August 1991, in final form 10 February 1992

Abstract. Two different kinds of assignment of energy levels for the Ti^{3+} ion and its local geometrical distortion in $BeAl_2O_4$ were suggested by experimental researchers. To check which is reasonable, first-principles calculations are performed on the electronic structure of Ti^{3+} with four cluster models. The study supports the energy-level diagram suggested by Sugimoto *et al*. A distorted configuration of the cluster $(TiO_6)^{9-}$ is proposed, with which experimental data can be satisfactorily explained and for which various electronic properties such as energy levels, density of states, orbital populations, charge distribution and spin polarization splitting are presented.

1. Introduction

Crystals activated with transition metal (TM) ions are attracting major attention because they can be used to construct tunable solid state lasers [1]. The dependence of the excited-level position of TM ions with the $d^3(Cr^{3+}, V^{2+})$, d^7 (Co^{2+}) and d^8 (Ni^{2+}) valence electron shell configuration on the internal crystal field in some host crystals has made it possible to use the electronic–vibrational transition to achieve frequency-tunable lasing action in the near- and middle-infrared ranges [2–5]. However, since ions of these types are usually characterized by absorption in the excited states at the pump and lasing frequencies, the efficiencies of lasers of these kinds are relatively low and the tuning range is limited. A decisive solution to this problem is provided by the doping of such crystals with ions with the d^1 or d^9 configurations $(Ti^{3+}, V^{4+}, Cu^{2+}$, etc) which do not exhibit this effect. This approach was first confirmed as promising by Moulton [6], where lasing due to transition in the Ti^{3+} ions in corundum ($Ti:Al_2O_3$) is demonstrated. Unlike other tunable solid state laser materials, this novel laser is characterized by a large gain cross section, a broad tuning range and the absence of excited-state absorption, and it can be pumped in many convenient ways. Extensive interest is then aroused in seeking out the newer tunable laser materials.

Recently, the lasing operation of Ti^{3+}-doped chrysoberyl ($Ti:BeAl_2O_4$) has also been demonstrated by Alimpiev *et al* [7] in the near-infrared range (0.73–0.95 nm). This new laser material was reported to have a longer photoluminescence lifetime (about 5 μs) than $Ti:Al_2O_3$ (3.1 μs) and is expected to have at least the same tuning range as $Ti:Al_2O_3$ does. Also, it does not suffer from severe parasitic absorption

0953-8984/92/225181+08$04.50

which exists in Ti:Al_2O_3 in the lasing as well as the ultraviolet ranges [8]. All these features make Ti:$BeAl_2O_4$ promising and attractive as one of the best tunable laser materials.

Chrysoberyl has an orthorhombic structure [9] with lattice constants $a = 9.404$ Å, $b = 5.476$ Å and $c = 4.427$ Å. It has two kinds of inequivalent Al^{3+} sites (C_s and C_i) for which the Ti^{3+} ions are expected to substitute. ESR measurements have shown, however, that nearly all [10] or at least 90% [7] of Ti^{3+} ions are located at C_s sites, so it is believed that only Ti ions at C_s sites are responsible for the lasing action in Ti:$BeAl_2O_4$ although some d–d transitions for Ti^{3+} ions at C_i sites can also be induced by odd-parity phonons. Two different kinds of assignment of energy levels for Ti^{3+} $3d^1$ at the C_s site have been suggested [10, 11]. Chiba *et al* [10] observed that their ESR signal reveals twofold symmetry, which implies that the substitutional Ti site may have a symmetry higher than C_s. They attributed such local lattice distortion to the fact that the ionic radius of the Ti^{3+} ion is 40% larger than that of the Al^{3+} ion [10] and proposed an energy-level diagram for Ti $3d^1$ under D_{2h} symmetry. On the other hand, Sugimoto *et al* [11] measured the detailed optical properties of Ti:$BeAl_2O_4$ and observed that both absorption and photoluminescence spectra show doublet peaks and strong anisotropy. They then proposed a possible energy-level diagram for Ti $3d^1$ under C_s symmetry. This diagram was constructed on the basis of group theory only and a quantitative analysis is needed to verify it. Thus, both the local geometry and the assignment of energy levels for the Ti ion are still undetermined, and these are important for a further understanding of the lasing action in Ti:$BeAl_2O_4$.

Aiming at resolving the above discrepancies, we performed a first-principles calculation on the electronic structure of Ti^{3+} in $BeAl_2O_4$ with four cluster models by the discrete variational DV–X_α method. This method is a kind of molecular-orbital calculation approach based on the local-density-functional theory. Since detailed descriptions of the method can be found elsewhere [12–14], in this paper we shall not give any more details. In the remainder of the paper, we shall first explain the choice of models and computational parameters in section 2, then present our results and discussion in section 3 and end with a summary in section 4.

2. Cluster models and computational parameters

The electronic structure of Ti^{3+} in $BeAl_2O_4$ can be obtained by calculations on the ionic cluster $(TiO_6)^{9-}$ made up of Ti^{3+} and its six nearest O^{2-} ions. Four models of this cluster are taken into account to discuss the energy-level diagram and local geometrical distortion. Model (A) (figure 1(*a*) and table 1) with C_s symmetry is taken according to Sugimoto *et al* [11], where Ti^{3+} is assumed to substitute for Al^{3+} at regular sites, without causing any local geometrical relaxation. In our choice of coordinate system, four O^{2-} ions (O(3), O(4), O(5) and O(6)) lie on a plane parallel to the x–y plane, forming an isosceles trapezium, and our y-axis is parallel to the b-axis in [9]. Model (B) (figure 1(*b*)) with D_{2h} symmetry is taken from the work of Chiba *et al* [10] who took the parameters of this cluster to be the average of corresponding sides of model (A), i.e. $\overline{TiO(1')} = \overline{TiO(2')} = \frac{1}{2}[\overline{TiO(1)} + \overline{TiO(2)}] =$ 3.59255 au, $\overline{O(3')O(4')} = \overline{O(5')O(6')} = \overline{O(3)O(4)} = \overline{O(5)O(6)} = 5.21002$ au and $\overline{O(3')O(6')} = \overline{O(4')O(5')} = \frac{1}{2}[\overline{O(3)O(6)} + \overline{O(4)O(5)}] = 5.17400$ au. It should be pointed out, however, that Chiba *et al* mistook $\overline{O(4)O(5)}$ for $\overline{O(3)O(4)}$ and vice

versa in their average procedure and hence obtained a set of parameters different from ours. For comparison, calculations are made for model (B) with both sets of parameters, denoted by model (B-1) for our choice and model (B-2) for the choice of Chiba *et al.* Based on the results of the above models, two more models, model (C) (table 1) and model (D), both with C_s symmetry are considered for a better understanding of the experimental data. The details will be given in section 3.

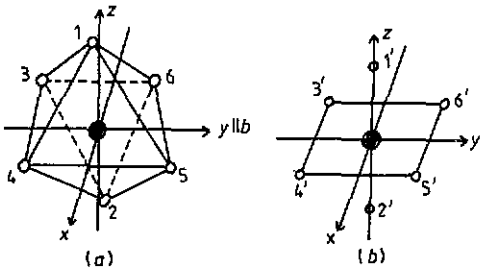

Figure 1. Geometrical configurations of cluster models (*a*) (A) and (*b*) (B): O, oxygen atoms; ●, titanium atoms.

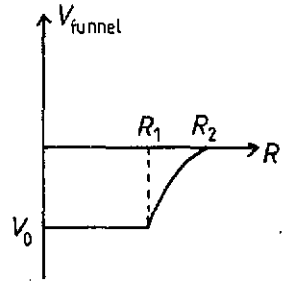

Figure 2. Funnel potential well.

Table 1. Coordinates of atoms in clusters (A) and (C) (in au).

	Model (A)			Model (C)		
	x	*y*	*z*	*x*	*y*	*z*
Ti	0.0	0.0	0.0	0.0	0.0	0.0
O(1)	0.02818	0.0	3.51779	0.02818	0.0	3.54500
O(2)	−0.55460	0.0	−3.62500	−0.55460	0.0	−3.59860
O(3)	−2.94086	−2.40922	−0.25987	−2.79239	−2.49811	−0.25987
O(4)	2.25701	−2.76478	−0.25987	2.45046	−2.67589	−0.25987
O(5)	2.25701	2.76478	−0.25987	2.45046	2.67589	−0.25987
O(6)	−2.94086	2.40922	−0.25987	−2.79239	2.49811	−0.25987

The spin-polarized scheme is adopted in our DV–X_α calculations. The variational basis set consists of the 1s–4p of the Ti^3 ion and the 1s–2p of the O^{2-} ion subjected to a funnel potential well (figure 2 and table 2) [15]. Lower-energy orbitals (1s–2p of Ti^{3+} and 1s of O^{2-}) are treated as frozen cores. A total number of 3000 Diophantine sampling points are used in the numerical integration. A charged Watson sphere with radius 5.5 au and charge 9.0*e* is taken to enclose the cluster so as to reflect in some degree the effect of the crystal environment and to keep the system electrically neutral. The convergence accuracy of our self-consistent charge process is 10^{-4}.

Table 2. Parameters for funnel potential well (in au).

	R_1	V_0	R_2
Ti^{3+}	3.0	−2.0	4.5
O^{2-}	3.0	−3.0	5.5

3. Results and discussion

3.1. Determination of a reasonable distorted cluster

Table 3 lists our main calculated results. The definitions of relevant parameters of the energy-level splittings for Ti^{3+} $3d^1$ in the table are illustrated in figure 3. The comparison of our results with experimental data is made in the following ways. Δ_1 and Δ_2 correspond to the absorption doublet peaks according to the Frank–Condon principle [16]. The values of δ_1 and δ_2 are compared with those obtained by Chiba *et al* [10], which were determined from their measured g-factors using Pryce's [17] static crystal-field formalism. Sometimes electron–lattice coupling effects are included when considering the level splitting of a degenerate ground electronic state. The Ham effect for $T_2 \times \epsilon$ in $Ti:Al_2O_3$ is an example [18]; the electron–lattice coupling Hamiltonian $H' = \sum_k (\partial V/\partial Q_{\epsilon_k})_{Q=0} Q_{\epsilon_k}$ reduces the off-diagonal matrix elements of H_{so} (spin–orbit coupling) or V' (non-cubic crystal-field), etc, within the ground cubic electronic term (T_2 triplet) by introducing vibrational Q_ϵ-mode instantaneous distortion of the lattice resulting in $T_2 \times \epsilon$ vibronic states; therefore this H' affects the level splitting of the T_2 state. For $Ti:BeAl_2O_4$, however, the site symmetry of the Ti^{3+} ion is far from cubic symmetry (the C_s symmetry term in the Hamiltonian H is quite large [19]) and the ground electronic state is the entirely non-degenerate A′ state. So H', which is effective within the ground electronic state, is only $(\partial V/\partial Q_{A'})_{Q=0} Q_{A'}$ under C_s symmetry, which keeps the A′-type symmetry of the equilibrium configuration. Although $H'' = (\partial V/\partial Q_{A''})_{Q=0} Q_{A''}$ can, in principle, couple A′ and A″ electronic states and produce A″-type instantaneous distortion of the lattice, its effects on the level splitting are negligible because the energies of the electronic states A′, A″, etc, are already well separated. Therefore, we calculate the energy structure within the static model and use the values of δ_1 and δ_2 obtained by Chiba *et al* as the experimental data in table 3.

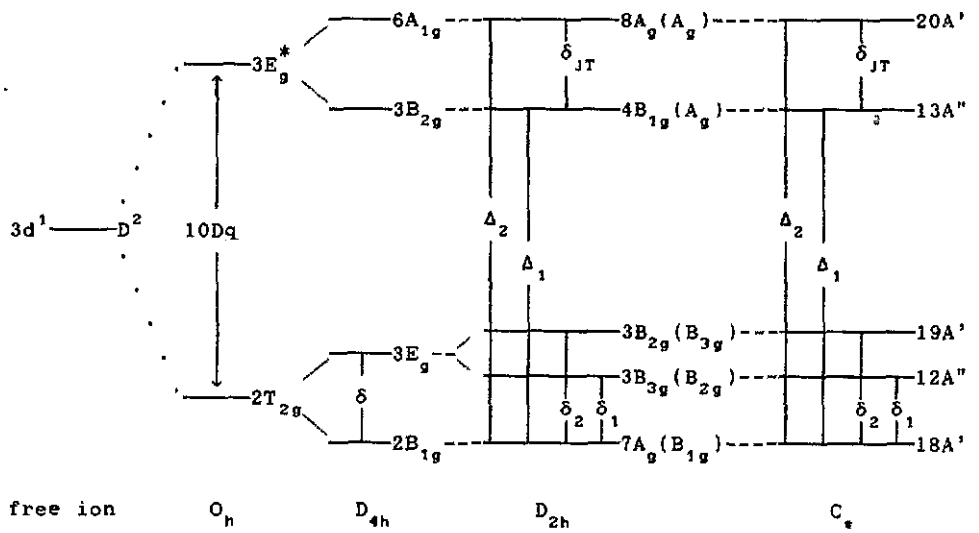

Figure 3. Schematic diagram of energy levels for Ti $3d^1$ in $BeAl_2O_4$.

Model (A) generates the energy levels for Ti^{3+} $3d^1$ in the same order as that suggested by Sugimoto *et al*, as shown in figure 3 and, from table 3, Δ_1, Δ_2 and

Table 3. A comparison of calculated energy-level splittings (in cm^{-1}) for Ti $3d^1$ in cluster models (A)–(D) with experimental data.

	Cal. (Models)					Exp.		
Splitting	(A)	(B-1)	(B-2)	(C)	(D)	[7]	[11]	[10]
δ_1	1142	273	582	998	1395	—	—	1060
δ_2	1714	277	2174	1341	1442	—	—	1280
Δ_1	17793	17678	16844	17936	17194	18250	17440	19000
Δ_2	20340	19671	21718	19897	19608	20120	19980	—
δ_{JT}	2546	1993	4874	1961	2413	1870	2540	—
$10Dq$	18115	18491	18362	18137	17456	18850	—	—

δ_{JT} agree well with the values found by Sugimoto *et al* and also by Alimpiev *et al*, but the splittings δ_1 and δ_2 from the low-lying $2T_{2g}$ are considerably greater than those found by Chiba *et al*. This indicates that the doping of Ti^{3+} causes some local geometrical distortion and this relaxation tends to heighten the symmetry at the Ti site so that the splittings δ_1 and δ_2 are reduced.

As the symmetry at the Ti site is enhanced from C_s to D_{2h}, however, δ_1 and δ_2 in model (B-1) become much smaller than the corresponding values for model (A) and the experimental values. This implies that the distortion is overestimated in model (B-1). Moreover, if the symmetry at the Ti site had really increased from C_s to D_{2h}, the Ti site would have inversion symmetry, and a rather weak intensity and little anisotropy should be revealed in the absorption and photoluminescence spectra because of the approximately forbidden electric-dipole transition selection rule, but this is contrary to the experimental observations [11]. So, model (B-1) suggested by Chiba *et al* cannot account for experiments. The result with model (B-2) is unreasonable too. Also Chiba *et al* made a second error in labelling their energy levels with the irreducible representation (IR) of the D_{2h} group (as shown in parentheses in our figure 3) since their IR notation does not match their choice of framework (XYZ) but, instead, correspond to another framework $(X'Y'Z)$ with X' axis rotated counterclockwise from the x axis by 45°.

It is worth mentioning that we have carried out analyses on the cluster $(TiO_6)^{9-}$ under two symmetry chains $O_h \supset D_{4h} \supset D_{2h} \supset C_{2v} \supset C_s$ and $O_h \supset D_{4h} \supset C_{4v} \supset C_{2v} \supset C_s$ and the corresponding parameters of these cluster models are taken as the appropriate average of model (A). It is found that the results of the thus-designed cluster models with symmetry higher than C_s all deviate greatly from the experimental data.

It is recognized from the above discussion that the cluster $(TiO_6)^{9-}$ will undergo some relaxation but its symmetry will remain C_s. Such a distorted cluster is found to be model (C) (table 1). This model is considered to be a certain intermediate configuration between models (A) and (B-1).

Calculation shows that the energy levels for Ti^{3+} $3d^1$ in model (C) are of the same order as in model (A); meanwhile the energy-level splittings Δ_1, Δ_2, δ_{JT}, δ_1 and δ_2 as a whole agree with the experimental data better than those for model (A) do.

Another possible distorted cluster model that we have considered is model (D), because McClure [20] once pointed out that, in a cubic crystal, the increase in ionic radius usually causes a radially outward displacement of ions around an impurity. We

consider the case where six O^{2-} ions displace equally and the best result occurs when the displacement is 0.03 au, but Δ_1 in this cluster is too small, and so is 10 Dq. We conclude that the most reasonable cluster is model (C) and its electronic structure will be presented next.

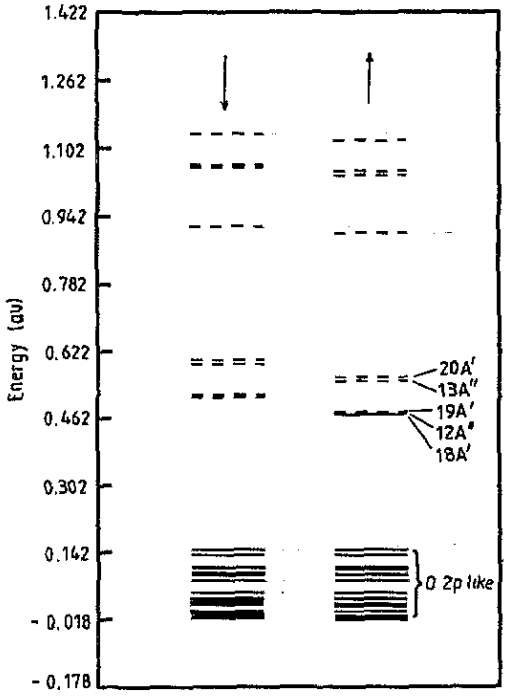

Figure 4. One-electron energy levels for cluster model (C) in the ground state: full curve, occupied orbital; broken curve, unoccupied orbital.

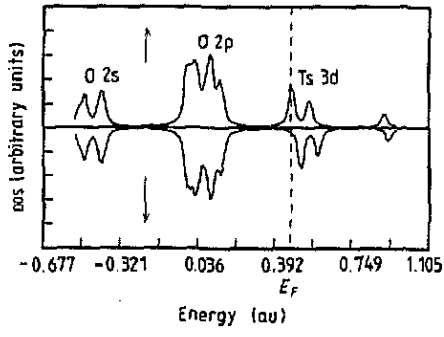

Figure 5. Density of states (DOS) for cluster model (C) ($EF = 0.4720$ au; $E_{min} = 0.677$ au; $E_{max} = 1.105$ au; $D_{min} = -180.000$; $D_{max} = 180.000$).

3.2. The electronic structure for model (C)

Figures 4 and 5 show the calculated one-electron energy levels and total density of states (TDOS), respectively, for model (C) in its ground electronic state. The TDOS in figure 5 is obtained by a Gaussian extension of the energy levels (the extension width is 0.015 au) [13], with each peak labelled by its dominant atomic orbitals. From figure 4, we see that the energy levels consist of the four following parts:

(1) below −0.3953 au are the O 2s non-bonding orbitals (omitted in the figure);
(2) between −0.0182 and 0.1472 au are the O 2p non-bonding orbitals;
(3) above 0.9020 au are the anti-bonding hybrids of Ti 4s, Ti 4p, O 2s, O 2p, etc;
(4) between 0.4697 and 0.5603 au are the Ti $3d^1$-dominated (75–93% in proportion) orbitals (called the crystal-field orbitals), which are distributed around the Fermi level (0.4720 au) and determine the character of the Ti^{3+} ion in the crystal.

Table 4. One-electron eigenvalues ϵ_i (in au) and orbital populations of crystal-field orbitals for model (C).

Orbital	$\epsilon_i(\uparrow)$	$\epsilon_i(\downarrow)$	Population ($\uparrow$)
18A′	0.4697	0.5126	0.93Ti 3d + 0.07O2p
12A″	0.4742	0.5171	0.92Ti 3d + 0.08O2p
19A′	0.4758	0.5189	0.92Ti 3d + 0.08O2p
13A″	0.5514	0.5921	0.77Ti 3d + 0.05O2s + 0.18O2p
20A′	0.5603	0.6000	0.75Ti 3d + 0.07O2s + 0.18O2p

The one-electron eigenvalues and orbital populations of the crystal-field orbitals are given in table 4. The transitions between these crystal-field levels have been shown earlier in table 3. It can be seen from table 4 that more mixings and hence more interactions exist between the Ti 3d electron and the ligands in the higher excited states 13A″ and 20A′ than in the lower energy levels 18A′, 12A″ and 19A′, resulting in a larger splitting δ_{JT} than δ_1 and δ_2. The absence of so-called excited-state absorption is understandable if one notices that the transitions associated with the lasing action are within the crystal-field levels while the other levels are located far from them. From figure 4, we see that the effect of spin polarization is negligible on the occupied non-bonding orbitals O 2s and O 2p but significant on Ti 3d-dominated and higher unoccupied orbitals, and we find from table 4 that the average splitting is 9194.7 cm^{-1} between corresponding spin-up and spin-down Ti 3d orbitals. A Mulliken population analysis (table 5) indicates that the effective charge of the Ti ion in $BeAl_2O_4$ is 2.5789e, markedly smaller than that of the free Ti^{3+} ion. This indicates there is a charge transfer of 0.4211e from the ligands to the Ti ion because of the molecular-orbital effect. Finally we find that the Ti ion has 1.02933 unpaired electrons in the cluster, which corresponds to a magnetic moment of 1.7658μ_B; this is in good agreement with the experimental value of (1.7–1.9)μ_B [16].

Table 5. Mulliken populations for atomic orbitals in model (C). EC and TNS denote the effective charge and total net spin of the ions in the cluster, respectively.

		Charge	Net spin			Charge	Net spin
Ti	3s	2.00740	−0.00049	O(1)	2s	1.99018	0.00004
	3p	6.03363	−0.00103		2p	5.94297	−0.00418
	3d	1.27502	1.03710				
	4s	0.02284	−0.00170	O(2)	2s	1.98693	0.00019
	4p	0.08220	−0.00455		2p	5.93416	−0.00443
O(3) or O(6)	2s	1.99301	−0.00012	O(4) or O(5)	2s	1.99138	−0.00020
	2p	5.94398	−0.00447		2p	5.92616	−0.00747

	Ti	O(1)	O(2)	O(3) or O(6)	O(4) or O(5)
EC	2.57890	−1.93315	−1.92109	−1.93698	−1.91754
TNS	1.02933	−0.00414	−0.00423	−0.00458	−0.00767

4. Summary

In this paper, we have performed first-principles calculations on the electronic structure of the Ti^{3+} ion in a $BeAl_2O_4$ crystal with four cluster models. Among them a

cluster model (C) is picked out, with which experiments can be explained better than with the undistorted cluster model (A) and others, and the energy levels, density of states, orbital populations and spin polarization splitting for model (C) are presented thereby.

Our calculations support the assignment of energy levels for Ti^{3+} $3d^1$ under C_s symmetry suggested by Sugimoto *et al* [11], except that our calculation expects some local relaxation which is inevitable within the C_s symmetry and that Sugimoto *et al* regarded the 12A'' level as closer to the lower 18A' level while our calculation shows that the 12A'' level is nearer to the higher 19A' level. Sugimoto *et al* drew this conclusion from their photoluminescence spectra which are related to the initial excited-electronic configuration while our conclusion is based on the ground electronic configuration. As is known in group theory, the magnitudes of splittings δ, δ_1 and δ_2 in figure 3 depend on the extent to which the octahedron distorts along the z, x and y directions, respectively. According to the measurements of g-factors based on the ground electronic configuration by Solntsev *et al* [21] and Chiba *et al* [10], g_x is closer to g_y and farther from g_z ($g_x = 1.710$, $g_y = 1.755$ and $g_z = 1.935$ in [10]); so distortion along the z direction is more severe than along the x and y directions, which results in a large splitting δ and a small $\delta_2 - \delta_1$; our results are thus reasonable. In addition, our calculations do not support the energy-level diagram proposed by Chiba *et al* [10] and two mistakes therein are pointed out.

Acknowledgment

This work is supported by the National Natural Science Foundation of China.

References

[1] Hammerling P, Budgor A and Pinto A 1985 *Tunable Solid State Lasers (Springer Series in Optical Sciences 47)* (Berlin: Springer)
[2] John L F and Guggenheim H J 1967 *J. Appl. Phys.* **38** 4837
[3] Moulton P F and Mooradian A 1978 *J. Opt. Soc. Am.* **68** 630
[4] Moulton P F and Mooradian A 1979 *Appl. Phys. Lett.* **35** 838
[5] Walling J C 1980 *IEEE J. Quantum Electron.* **QE-16** 1302
[6] Moulton P F 1986 *J. Opt. Soc. Am.* B **3** 125
[7] Alimpiev A I, Bukin G V, Matrosov V N, Pestryakov E V, Solntsev V P, Trunov V I, Tsvetkov E G and Chebotaev V P 1986 *Sov. J. Quantum Electron.* **16** 579
Pestryakov E V, Trunov V I and Alimpiev A I 1987 *Sov. J. Quantum Electron.* **17** 585
[8] Sanchez A, Strauss A J, Aggarwal R L and Fahey R E 1988 *IEEE J. Quantum Electron.* **QE-24** 995
[9] Farrel E F, Fang J H and Newnhaw R E 1963 *Am. Mineral.* **48** 804
[10] Chiba Y, Yamagishi K and Ohkura H 1988 *Japan. J. Appl. Phys.* **27** L1929
[11] Sugimoto A, Segawa Y, Kim P H, Namba S, Yamagishi K, Anzai Y and Yamaguchi Y 1989 *J. Opt. Soc. Am.* B **6** 2334
[12] Ellis D E and Painter G S 1970 *Phys. Rev.* B **2** 2887
[13] Ellis D E, Benesh G A and Byrom E 1979 *Phys. Rev.* B **20** 1198
[14] Ellis D E, Guenzburger D and Jansen H B 1983 *Phys. Rev.* B **28** 3697
[15] Xia Shang-Da, Guo Chang-Xin, Lin Li-Bin and Ellis D E 1987 *Phys. Rev.* B **35** 7671
[16] Griffith J S 1961 *The Theory of Transition-Metal Ions* (Cambridge: Cambridge University Press)
[17] Pryce M H 1950 *Proc. Phys. Soc.* A **63** 25
[18] Macfarlane R M, Wong J Y and Sturge M D 1968 *Phys. Rev.* **166** 250
[19] Liu Shi-Yu and Xia Shang-Da 1989 *Chinese J. Chem. Phys.* **2** 284
Liu Shi-Yu and Xia Shang-Da 1991 *Sci. Sinica* A **3** 271 (in Chinese)
[20] McClure D S 1962 *J. Chem. Phys.* **36** 2757
[21] Solntsev V P, Matrosov V N and Tsvetkov E G 1982 *J. Appl. Spectrosc.* **37** 1319